

Retrieval of mixing height and dust concentration with lidar ceilometer

Christoph Münkkel · Noora Eresmaa ·
Janne Räsänen · Ari Karppinen

Received: 1 December 2005 / Accepted: 12 June 2006 / Published online: 5 August 2006
© Springer Science+Business Media B.V. 2006

Abstract The Vaisala ceilometers CT25K and CL31 are eye-safe single lens lidar systems reporting attenuated backscatter profiles; they often operate 24 h a day in fully automated, hands-off operation mode. These profiles can be used for more than just cloud-base height determination. In dry weather situations, there is a fairly good correlation between the ceilometer near-range backscatter and in situ PM10 concentration readings. The comparison of mixing height values based on soundings and on ceilometer backscattering profiles indicates that ceilometers are suitable instruments for determining the convective mixing height. Its enhanced optics and electronics enables the CL31 ceilometer to detect fine boundary-layer structures whose counterparts are seen in temperature profiles.

Keywords Aerosol · Ceilometer · Lidar · Mixing height

1 Introduction

Lidar (“light detection and ranging”) is an active range-resolving optical remote measurement technique. Commercial lidar ceilometers have to date been mainly installed at airfields and meteorological stations to report cloud layers, vertical visibility, and cloud cover (Weitkamp 2005, pp 175–181). Additionally, their regular boundary-layer scans can be examined for the retrieval of parameters such as extinction coefficient profiles, visibility mixing height, and dust concentration. Being constructed to operate

C. Münkkel (✉)
Vaisala GmbH, Schnackenburgallee 41d, 22525 Hamburg, Germany
e-mail: christoph.muenkel@vaisala.com

N. Eresmaa · A. Karppinen
Finnish Meteorological Institute, Helsinki, Finland

J. Räsänen
Vaisala Oyj, Vantaa, Finland

permanently and unattended for several years in all kinds of meteorological environment qualifies these eye-safe instruments also for air quality surveillance purposes.

2 Ceilometer basics and technical properties

2.1 Simplified lidar equation

The optical power received by a ceilometer from distance x is

$$P(x, \lambda) = \frac{c}{2x^2} \underbrace{P_0 A \eta O(x) \Delta t}_{\text{instrument specific}} \times \underbrace{\beta(x, \lambda) \tau^2(x, \lambda)}_{\text{attenuated backscatter}}, \quad (1)$$

where c is the speed of light, Δt is the (laser) pulse duration, P_0 is the average laser power during the pulse, A is the area of the receiver optics and η is its efficiency. $O(x)$ is the range-dependent overlap integral between the transmitted beam and the field-of-view of the receiver (complete overlap at $O(x) = 1$). $\beta(x, \lambda)$ is the backscatter coefficient, $\tau(x, \lambda)$ is the transmittance of the atmosphere between the lidar and the scattering volume, λ is the wavelength of the emitted laser pulse, and x is the distance between lidar and scattering volume.

After solving for all the instrument specific factors, constants and squared distance, the attenuated backscatter coefficient can be retrieved. This quantity is the product of the volume backscatter coefficient β at range x and the square of the transmittance of the atmosphere between the lidar and the scattering volume τ^2 .

During all cases with range values x above 30 m discussed in this paper, the meteorological optical range at ground level exceeded 10,000 m, leading to τ^2 values that are greater than 0.83. This is reasonably close to 1 to take the attenuated backscatter coefficient as a measure for β . If we further assume that the scatterer properties remain unchanged through the sample volume, the backscatter values would also correlate with the range-resolved aerosol concentration. Correspondingly, having the scatterer properties at a certain height constant with time would enable seeing temporal variations in aerosol concentration in a selected volume.

2.2 Optical ceilometer designs

The instrument involved in the measuring campaigns treated in Sect. 3 and Sect. 4.2.1 is the Vaisala ceilometer CT25K, which is a single lens lidar system equipped with pulsed near-infrared diode lasers. To obtain sufficient signal-to-noise ratios, the return signal of 65,000 laser pulses is integrated for each range gate. A beam splitter gives full overlap of the transmitter and receiver field-of-view already at an altitude of 0 m. Direct reflections at the lens surfaces give a high signal at the receiver. To prevent receiver saturation by this strong cross-talk signal between transmitter and receiver, compensation electronics are used with an optical fibre feeding the negative amount of the transmitter signal to the receiver. Figure 1 contains a schematic arrangement of the CT25K optical concept.

The latest Vaisala ceilometer CL31 (Fig. 2) uses a novel single lens design, whose main innovation is in the way the common lens is used for transmitting and receiving light. The centre of the lens is used for collimating the outgoing laser beam, whereas the outer part of the lens is used for focusing the backscattered light onto the receiver.

Fig. 1 Optical concept of the single lens lidar ceilometer CT25K

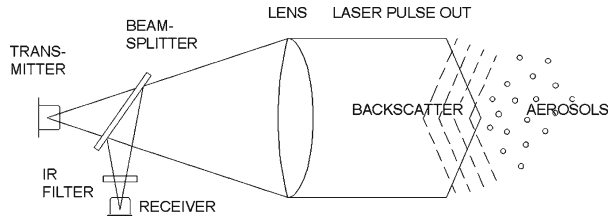


Fig. 2 Ceilometer CL31, overall height = 1190 mm



The division between transmitting and receiving areas is provided by an inclined mirror with a hole in the centre as shown in Fig. 3. This arrangement significantly reduces the optical cross-talk between transmitter and receiver. The need for separate compensation mechanisms is avoided leading to a simpler and more reliable instrument design. The new single lens design is also robust against changes in the mechanical alignment of the optical parts. Measurement examples obtained with the CL31 ceilometer are presented in Sects. 4.2.2 and 4.2.3.

Fig. 3 Enhanced single lens optical concept of the lidar ceilometer CL31

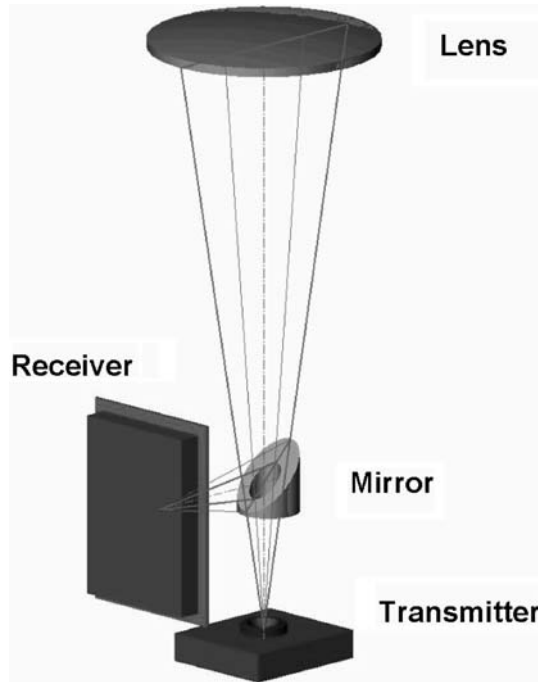


Table 1 Technical properties of the ceilometers CT25K and CL31

	CT25K	CL31
Measurement range (m)	0 – 7500	0 – 7500
Resolution (m)	15	10
Laser system	InGaAs MOCVD laser diode	InGaAs MOCVD laser diode
Wavelength (nm)	905	905
Pulse properties	100 ns, 1.6 μ J/pulse	110 ns, 1.2 μ J/pulse
Mean pulse repetition rate (Hz)	4369	8192

2.3 Ceilometer technical properties

Table 1 lists the main technical properties of the two lidar ceilometers used for this study. Eye-safety considerations do not allow larger single pulse energy values; this disadvantage is overcome by using high pulse repetition rates increasing the signal-to-noise ratio.

3 Aerosol concentration measurements

One task within the VALIUM measuring campaign carried out at the site of the Lower Saxony State Agency for Ecology (NLÖ) in Hanover, Germany, was the comparison of ceilometer near-range backscatter data with PM₁₀ and PM_{2.5} concentration reported half-hourly by point sampling sensors. Figure 4 shows the measurement set-up, where the PM₁₀ and PM_{2.5} inlet probes were situated 20 m above the ceilometer level.

Fig. 4 Measurement set-up for ceilometer aerosol concentration measurements, PM10 and PM2.5 inlet probes level is 20 m above the ceilometer



For comparison with in situ dust concentration, CT25K ceilometer attenuated backscatter from the two lowest range gates covering the elevation interval from 0 to 30 m has been averaged over a period of 30 min. Wet haze, fog, and precipitation situations were excluded from the data analysis by using only those 30-min intervals with relative humidity values below 62% and no precipitation detected. The latter information was provided by an optical yes/no precipitation monitor. 75.5% of all datasets gathered during the period between 1 March 2002 and 23 April 2003 were thus eliminated. The remaining 5736 “dry” datasets show a fairly good correlation ($R = 0.8351$) between the PM10 in situ concentration values and the average attenuated ceilometer backscatter β_{30} (Fig. 5). Raising the 62% relative humidity limit decreases the correlation quality ($R = 0.8138$ for a 74% limit, $R = 0.7730$ for a 86% limit); a smaller limit brings no significant quality increase. Assuming a linear relationship between β_{30} and PM10 concentration values, a correlation analysis gives a simple equation for the estimation of PM10 concentration ρ_{PM10} with a ceilometer. The resulting linear fit coefficients are $m = 2.023 \times 10^7 \mu\text{g m}^{-2} \text{ sr}$ and $b = -1.6304 \mu\text{g m}^{-3}$,

$$\rho_{\text{PM10}} = m\beta_{30} + b. \quad (2)$$

Figure 6 shows the comparison of PM10 concentration derived from ceilometer data with in situ values for a fair weather period. The in situ measured PM2.5 concentrations

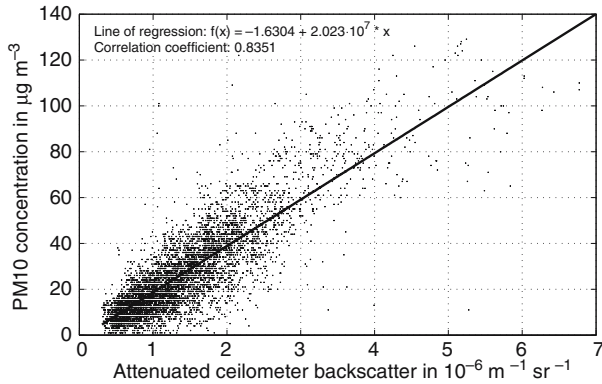


Fig. 5 Ceilometer attenuated backscatter versus in situ measured PM10 concentration, 5736 dry weather datasets, NLO Hanover, 1 March 2002–23 April 2003

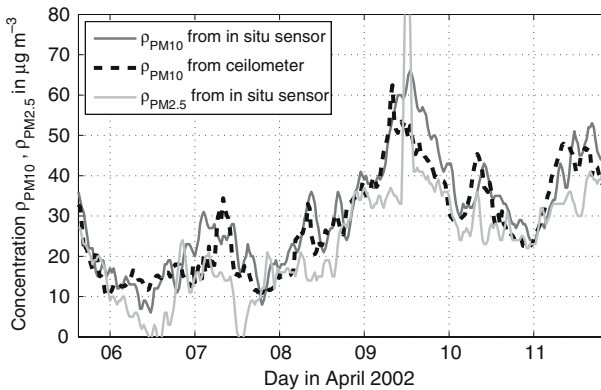


Fig. 6 PM10 and PM2.5 concentrations reported from in situ sensors and ceilometer, NLO Hanover, April 2002

are also plotted. In some instances these exceed the PM10 values; this is not reasonable because PM10 concentration includes all particles with sizes ranging from $0\ \mu\text{m}$ to $10\ \mu\text{m}$ and should therefore not be smaller than the concentration of all particles below $2.5\ \mu\text{m}$. This finding illustrates that the 30-min averaging interval for in situ PM assessment is a challenge for PM measurements in general.

4 Mixing height retrieval

4.1 Methods

As it was stated in Sect. 2, we can expect the lidar backscatter profiles to track the aerosol concentrations in a reasonably transparent atmosphere. The aerosol concentrations, in turn, can be expected to reveal details about the vertical structure of the atmospheric boundary layer, such as mixing height.

Generally, a number of methods for retrieving mixing layer height from lidar backscatter profiles have been presented (Menut et al. 1999; Steyn et al. 1999; Cohn and Angevine 2000; Davis et al. 2000).

The known methods are mostly based on two assumptions about the atmospheric distribution of scattering aerosols. Firstly, the mixed layer is expected to have a somewhat constant concentration that is higher than in the layers above. Consequently, the difference between the mixed layer and the air above is assumed to be seen as a shift from a relatively strong backscatter inside the mixed layer to a lower backscatter level above it (Steyn et al. 1999). The methods used in this study are the so-called gradient method and the idealised backscatter method introduced by Steyn et al. (1999).

It must be emphasized, however, that not in all cases do lidar backscatter methods provide a good measure of the mixing height. During late afternoon when the planetary boundary layer is collapsing, the aerosol concentrations remain high and show the maximum depth of the daytime mixed layer. The aerosol concentration trace in nocturnal surface inversions is often too weak and dominated by high residual layers, as is the morning growth of the mixed layer. Examples will be discussed in Sect. 4.2.

4.1.1 Idealised backscatter method

The method relies on the assumptions mentioned above. The technique is based on fitting an idealised backscatter profile $B(z)$ to the measured attenuated backscatter profile $\beta(z)$ (see Fig. 7b). Fitting parameters include mean mixed layer backscatter B_m , mean backscatter immediately above the mixed layer B_u as well as mixing height itself and a measure s proportional to the entrainment zone thickness (Steyn et al. 1999),

$$B(z) = \frac{B_m + B_u}{2} - \left(\frac{B_m - B_u}{2} \right) \operatorname{erf} \left(\frac{z - \text{MH}}{s} \right). \quad (3)$$

The fitting procedure results in a mixing height estimate and a value characterising the entrainment zone.

4.1.2 Gradient method

The gradient method selects the maximum of the negative gradient ($-d\beta/dx$) of the backscatter coefficient to be the top of the mixed layer. To reduce sensitivity to noise and temporary details in atmospheric structure, vertical and temporal averaging may be applied before or after differentiation. Also, there are options of using either absolute maximum or local maxima for boundary-layer characterisation.

4.2 Measurements and results

4.2.1 One year campaign in Vantaa, Finland

The data used in this section were obtained on the premises of Vaisala Oyj, Vantaa (suburban Helsinki), Finland between 16 December 2001 and 10 November 2002 with a CT25K ceilometer. In convective situations, mixing height (MH) is estimated from radiosoundings using the Holzworth method—this follows the dry adiabatic starting at the surface up to its intersection with the temperature profile. In stable situations the Richardson number method (Joffre et al. 2001) is used, with a critical value of 1.

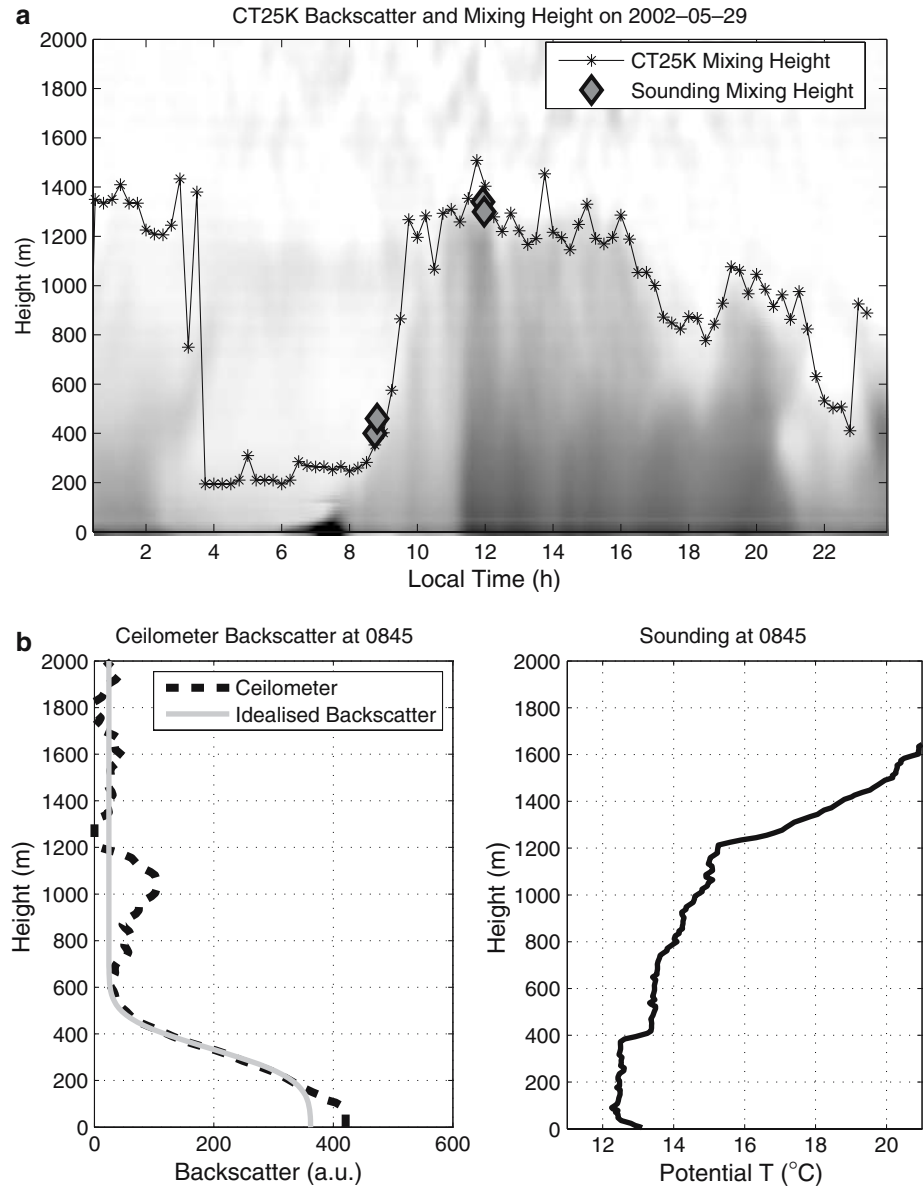


Fig. 7 Ceilometer and radiosounding data from Vaisala test field in Vantaa, suburban Helsinki, Finland on 29 May 2002. The backscatter image (**a**) includes the mixing height retrieved with the idealised backscatter method and mixing height computed from the radiosounding data. A snapshot at 0845 (**b**) confirms the match between ceilometer and sounding in more detail

The MH is determined from the ceilometer attenuated backscatter profile using the idealised backscatter method. In the fitting half-hourly averaged profiles have been used. A 24-h period of ceilometer observations is displayed in Fig. 7a. The method locates the boundary-layer top consistently on the clear spring day in question. The calculated mixing height is apparently reported to the residual layer height until about 0330 because trends in backscatter decrease with height are rather weak. After that, a stable layer with mixing height around 200 m is reported. Unfortunately, there are no radiosonde soundings available from the night to confirm if ceilometer data correctly report the conditions.

After sunrise, a convective boundary layer develops, eventually reaching about 1,300 m. There were four radiosoundings made on this day (see Fig. 7a) and they show very good agreement with the ceilometer mixing height. The increased backscatter at 11:30 local time may be connected to the start of the sea breeze from the direction of downtown Helsinki. It is readily seen how turbulence becomes stronger and the MH grows after the sun rises. The mixing height values after 23:00 local time show the residual layer.

A comparison between the mixing heights measured by the ceilometer and radiosoundings during the one year measuring campaign is shown in Fig. 8. A total of 71 convective and 38 stable clear sky cases were analysed. In convective situations 15 observations, and in stable situations a single observation, were rejected because of low backscattering signal near the surface (observations marked with a circle in Fig. 8), involving both the measured backscatter and the fitted B_m values from Eq. (3). A regression line is fitted to the remaining observations (stars in Fig. 8). The regression lines and correlation between MHs determined by ceilometer and soundings are listed in Table 2; the error margins in Table 2 correspond to 95% confidence level of the regression coefficients.

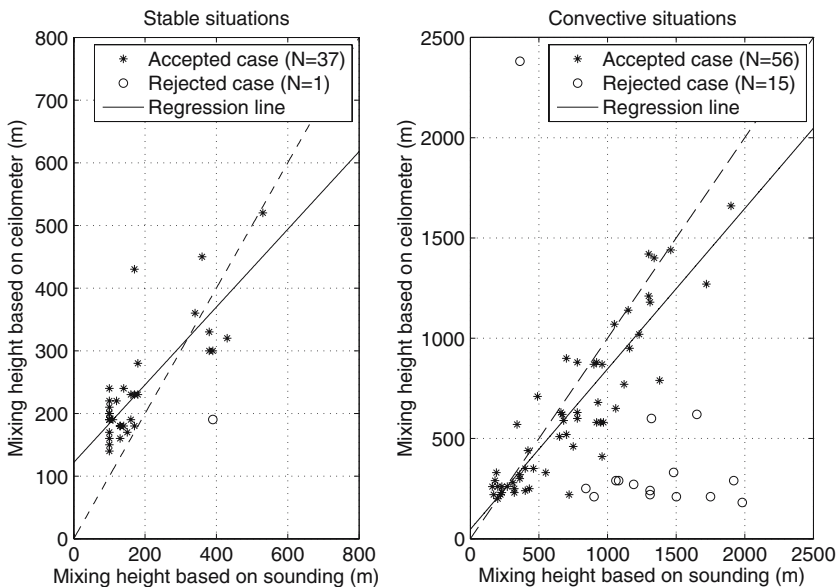


Fig. 8 Correlation between ceilometer and radiosounding MH

Table 2 Correlation and regression between MHs determined by ceilometer and soundings

	Correlation between ceilometer and sounding	Regression ($x = \text{MH}$ by ceilometer $y = \text{MH}$ by sounding)	Number of accepted cases	Number of rejected cases
Convective situations	0.9	$x = (0.8 \pm 0.1)y + (47 \pm 89)$	56	15
Stable situations	0.8	$x = (0.62 \pm 0.15)y + (124 \pm 32)$	37	1

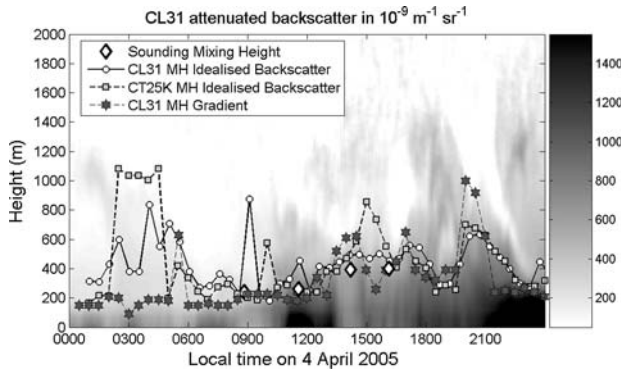


Fig. 9 Sliding average (150 m, 15 min) CL31 ceilometer attenuated backscatter profiles recorded in Vantaa, Finland on 04 April 2005 together with mixing heights determined by ceilometers and soundings. Residual layers are visible up to a height of 1,800 m

4.2.2 Inter ceilometer comparison for one day

Figure 9 shows a diurnal boundary-layer cycle on a nearly cloudless day, and contains attenuated backscatter profiles measured with the CL31 ceilometer and mixing heights calculated with the idealised backscatter method for both the CT25K and CL31, together with available radiosounding MHs for that day. Additionally, a gradient method that selects the absolute maximum of the negative gradient as the mixing height has been applied to the CL31 data. In most cases, this method shows a tendency to smaller mixing height values, with a decreased probability of reporting the height of the residual layer.

4.2.3 Boundary-layer structures and temperature inversions

The improved measurement performance of the CL31 ceilometer sharpens the view on structures in aerosol density. This can be studied using measurements made in a rural (Fig. 10) and an industrial environment (Fig. 11). Temperature inversion heights from radiosoundings are also plotted in Fig. 10. They are very close to local minima of the gradient of the attenuated backscatter profile. Stratification expected from the temperature profiles seem to accurately correspond to aerosol structures revealed in

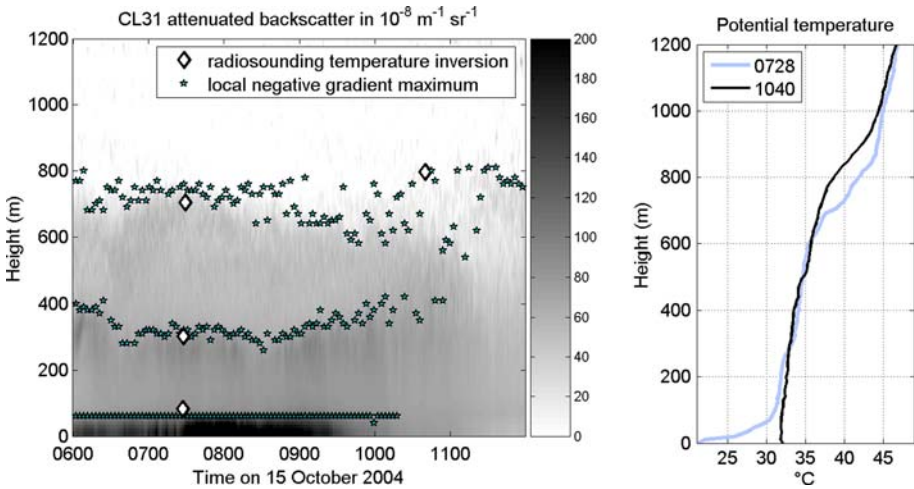


Fig. 10 Attenuated backscatter sliding average (50 m, 90 s) density plot recorded in Vantaa, Finland on 15 October 2004. For additional reference, potential temperature profiles from the soundings at 0728 and 1040 local time are shown

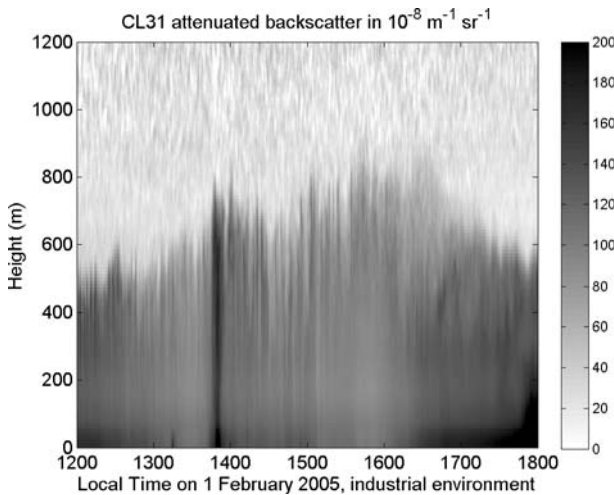


Fig. 11 Attenuated backscatter sliding average (50 m, 90 s) density plot recorded in Hamburg, Germany on 01 February 2005

backscatter profiles. The scattering aerosols are tracers of the prevailing atmospheric condition, and therefore produce a readable signature.

The upper edge of the boundary layer is very clearly visible in Fig. 11, and no further calculation is necessary to retrieve the mixing height.

When the gradient method is used in a way that selects the absolute maximum of the negative gradient of the attenuated backscatter coefficient as the mixing height, the highest local maxima from Fig. 10 are picked as the mixing height, except for the time interval from 0725 to 0850, when the first maximum at 50 m is chosen.

5 Summary and conclusions

Ceilometers are affordable, reliable, and essentially maintenance free tools for mixing height assessment and boundary-layer scans in clear sky cases.

A promising algorithm for dust particle concentration measurements with ceilometers has been developed, though further studies incorporating the new ceilometer CL31 are required for its refinement and finalisation, and for testing its ability to obtain vertical concentration profiles. Special attention has to be paid to the correct identification of weather situations that rule out the applicability of this approach. A measuring campaign close to a meteorological mast should be performed to investigate the influence of the relative humidity profile.

Ceilometers show promising performance and take a step towards automated mixing height measurement. The results indicate that applying the idealised backscatter method to ceilometer data works for both stable and unstable conditions. The gradient method extracts significant information from the profiles. A matter for further studies would be, e.g., comparing the methods against a reference such as frequent radiosoundings, SODAR, windprofiler, or RASS measurements.

References

- Cohn SA, Angevine WM (2000) Boundary-layer height and entrainment zone thickness measured by lidars and wind-profiling radars. *J Appl Meteorol* 39:1233–1247
- Davis KJ, Gamage N, Hagelberg CR, Kiemle C, Lenschow DH, Sullivan PP (2000) An objective method for deriving atmospheric structure from airborne lidar observations. *J Atmos Oceanic Tech* 17:1455–1468
- Joffre SM, Kangas M, Heikinheimo M, Kitaigorodskii SA (2001) Variability of the stable and unstable Boundary-layer height and its scales over a Boreal Forest. *Boundary-Layer Meteorol* 99:429–450
- Menut L, Flamant C, Pelon J, Flamant PH (1999) Urban Boundary-layer height determination from lidar measurements over the Paris Area. *Appl Optics* 38:945–954
- Steyn DG, Baldi M, Hoff RM (1999) The detection of mixed layer depth and entrainment zone thickness from lidar backscatter profiles. *J Atmos Oceanic Tech* 16:953–959
- Weitekamp C (Ed.) (2005) *Lidar: range-resolved optical remote sensing of the atmosphere*, Springer, New York, 460 pp